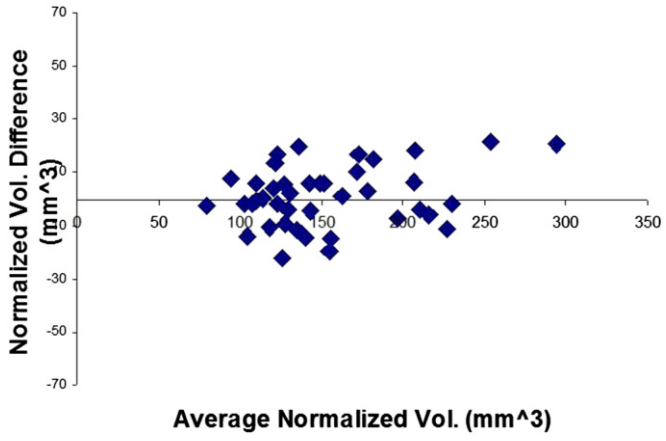

Fig. 2. Medial Compartment (BL - 12 mo).

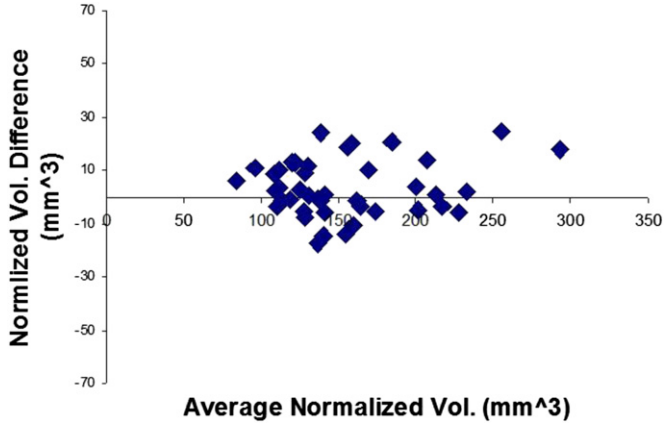

Fig. 3. Medial Compartment (BL - 48 mo).

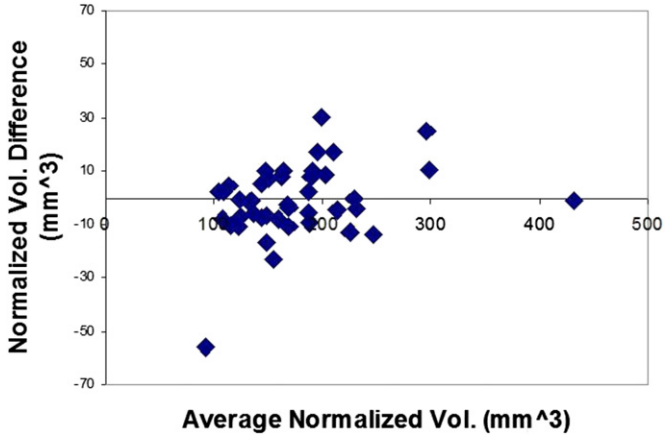

Fig. 4. Lateral Compartment (BL - 12 mo).

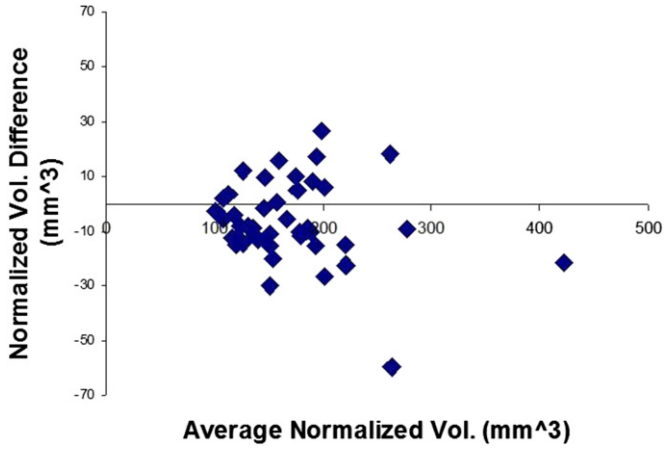

Fig. 5. Lateral Compartment (BL to 48 mo).

375

ACCURACY OF HIGH RESOLUTION ULTRASONOGRAPHY IN DETECTING MENISCAL TEARS

Y. Akatsu, S. Yamaguchi, T. Sasho, K. Takahashi, R. Akagi, Y. Muramatsu, J. Katsuragi, T. Fukawa, S. Mukouyama, J. Endo. *Chiba Univ., Chiba, Japan*

Purpose: MRI is the first-line modality to diagnose meniscal pathology. Possible alternative to MRI is an ultrasound scanning which is quick to perform and less costly. The aim of this study was to assess the accuracy of high resolution ultrasonography in the diagnosis of meniscal tears with arthroscopic examination as standard reference.
Methods: Fifty pair of menisci were evaluated in 50 patients (23 females, 27 males, mean age = 32.5 years, range = 13-80 years). Knee examinations were performed with high resolution ultrasonography machine (Hi Vision Preirus, Hitachi, Japan) with 8-14 MHz linear transducer. Inclusion criteria for the study were 1) knees that needed to be treated or examined arthroscopically due to intra articular pathology, and 2) unilateral involvement. Exclusion criteria were a history of rheumatoid arthritis or other inflammatory disease, peri-articular fracture, Paget's disease, joint infection, neuropathic arthropathy, acromegaly, gout, and pseudogout. Examiner was not informed preoperative diagnosis and laterality. After ultrasonographic examination, all patients underwent arthroscopic procedures within 1-3 days. After the final diagnosis about meniscal status was derived from surgical reports, ultrasonographic diagnosis was compared in terms of presence of tear as well as type of tear when tears were present.
Results: The overall sensitivity, specificity, positive predictive value, and negative predictive value of ultrasonographic examination in the assessment of meniscal tears amounted to 90%, 70%, 92% and 64%, respectively. The statistical parameters were not statistically different in medial and lateral menisci. Sensitivity, specificity, positive predictive value and negative predictive value of ultrasonographic examination in the assessment of medial meniscal tears vs. lateral meniscal tears were 96% vs. 65%, 74% vs. 88%, 81% vs. 81%, and 94% vs. 76%, respectively. As for diagnostic ability in diagnosing the type of meniscal tear, the sensitivity and positive predictive value of horizontal tear, vertical tear, radial tear, flap tear, bucket handle tear, complex tear, discoid were 71% vs. 36%, 47% vs. 58%, 0% vs. 0%, 40% vs. 67%, 55% vs. 86%, 88% vs. 54%, 100% vs. 100%. Age, sex, body mass index (BMI), weight, did not have a statistically significant impact on the usefulness of ultrasonography.
Conclusions: High resolution ultrasonography had high accuracy in the detecting the presence of tears both in medial and lateral menisci. But type of meniscal tear was difficult to diagnose.

376

AUTOMATIC SEGMENTATION OF ARTICULAR CARTILAGE FROM COMBINED ASSESSMENT OF SODIUM AND PROTON MR KNEE IMAGES

A. Mohd Hani[†], D. Kumar[†], A. Malik[†], N. Walter[†], R. Razak[‡], A. Kiflie[§]. [†]*Ctr. for Intelligent Signal and Imaging Res., Universiti Teknologi Petronas, Tronoh, Malaysia;* [‡]*Orthopaedic Dept., Hosp. Pantai Ipoh, Ipoh, Malaysia;* [§]*Dept. of Radiology, Hosp. Pantai Ipoh, Ipoh, Malaysia*

Purpose: Articular cartilage (AC) segmentation from magnetic resonance images of knee joint play a major role in quantifying morphological and physiological changes during the onset of osteoarthritis (OA). Prior research in cartilage segmentation has shown difficulties to develop fully automatic method due to heterogeneous AC signal, low tissue contrast, uneven shape and complex behaviour. This work aims to develop an automated AC segmentation technique utilizing combined assessment of sodium and proton MR images acquired at 1.5T.

Methods: MR scans of human knee were performed at 1.5T using a dual tuned knee coil (23Na/1H- tuned at 63.6 MHz for proton and 16.8 MHz for sodium nuclei) without changing the position of knee/coil. High resolution proton images are acquired using 3D MEDIC (TR/TE =37/20 ms, image resolution = 0.47x0.51x1.5mm3 and 48 slices) while sodium images are acquired using 3D Gradient Echo (TR/TE=11.4/ 4.0 ms, image resolution = 2.81x2.81x 8mm3, and 12 slice). Sodium rich region from the sodium MR slices are extracted using a method developed by our group earlier. Extracted sodium region slices were re-sampled using cubic spline interpolation followed by the normalization that was then merged with corresponding proton slices. Results obtained from fusion shows an enhanced cartilage region in fused slices. Cartilage region from fused images were manually segmented by an expert. For the automatic segmentation, the contrast of fused image was enhanced by applying histogram equalization that adjusts the signal intensities as the pixel intensities >250 values are excluded. Once the image is enhanced, all the connected components in the image are selected and property of image region as convex area is measured followed by the detection of edges in all existing objects within the image. This results in a single object as articular cartilage region from the fused slice. The same procedure is repeated to segment the cartilage region from all the slices in one dataset. Automatically segmented cartilage regions are compared with the cartilage region obtained from the manual segmentation performed by an expert.

Results: The results as shown in Figure 1 (a) represents a single slice of a dataset containing proton MR images and Figure 1(b) represents a slice of sodium MR image of knee at same location. Figure 1(c) shows extraction of sodium region from sodium image which were then merged with original corresponding proton MR slice as shown in Figure 1 (e). For the automatic segmentation of AC, contrast of fused images were enhanced as shown by an example in Figure 1 (f) followed by the exclusion of pixel intensities values >250 as shown in Figure a (g).

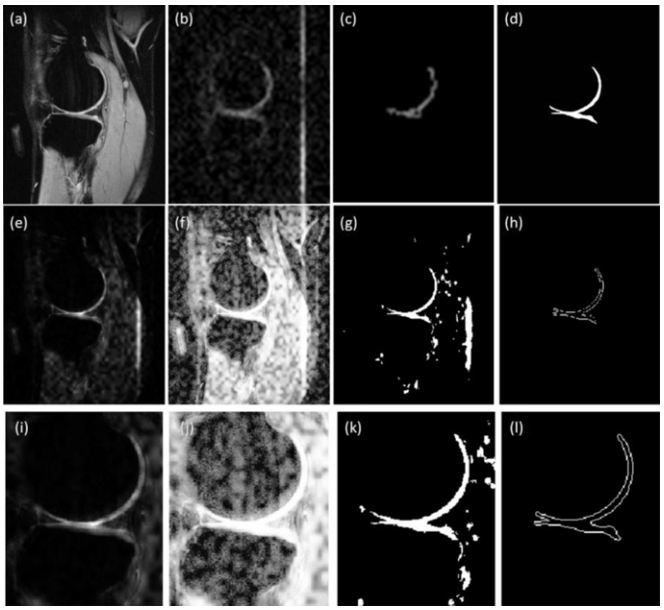

Figure 1. Representation of steps followed to segment AC automatically using combined assessment of proton and sodium MR images of knee: (a) Original Proton knee Image, (b) Original sodium knee image, (c) sodium extracted region from sodium knee MR image, (d) manually segmented articular cartilage, (e) Merged sodium and proton image, (f) output from contrast enhancement in merged image, (g) image with region excluding pixel intensities >250, (h) automatically segmented AC. Figure (i), (j), (k) and (l) showing the automatic segmentation steps at higher scale.

Finally, the image region as convex area is measured from the resulting images which were then used to detect the edges on the available objects that give a single cartilage region as segmented area as shown in Figure 1 (h). Figure 1 (i, j, k and l) shows the visualisation of same steps as in Figure 1 (e, f, g and h) at higher scale. An expert was asked to manually segment the AC in fused images. Total of 126 images from 3 datasets were manually segmented as shown in Figure 1(d) that takes approximately 3 hours 40 minutes. The results of automatic segmentation of articular cartilage achieved average sensitivity and specificity of 80.27% and 99.65% respectively.

Conclusions: In this study, AC is segmented automatically from the combined assessment of sodium and proton MR images that shows applicability of this method to quantify cartilage changes during the OA progression. Sensitivity and specificity of 80.27% and 99.65% respectively achieved from the comparison of automatic and manual segmentation in this work matches to semi-automated and few automated methods reported earlier.

377
ADVANCED IMAGE ANALYSIS AND FINITE ELEMENT MODELING FOR KNEES WITH OSTEOARTHRITIS

W.-C. Lo [†], L. Ge [‡], R.B. Souza [†,§], X. Li [†]. [†] *Dept. of Radiology and BioMed. Imaging, Univ. of California, San Francisco, San Francisco, CA, USA;* [‡] *Div. of Adult Cardiothoracic Surgery, Univ. of California, San Francisco, San Francisco, CA, USA;* [§] *Dept. of Physical Therapy and Rehabilitation Sci., Univ. of California, San Francisco, San Francisco, CA, USA*

Purpose: Finite element (FE) models have been used to analyze cartilage deformation and kinematic changes of human knees with osteoarthritis. However, no studies have yet used in-vivo imaging data to approximate material properties of the cartilage, and no research has compared the FE output using subject-specific material properties with in-vivo measurements of cartilage. The goals of this research are (1) to develop a novel subject-specific FE model using in-vivo T1ρ and morphological data from high-resolution MRI; (2) to compare the tissue deformation of cartilages and contact area in an FE model using T1ρ and morphology with unloaded and loaded MR data.

Methods: One mild OA patient was scanned using a 3T GE Signa MR Scanner with an 8-channel phased-array knee coil. The 3D FSE (CUBE) high resolution images (0.5 mm isotropic voxel) under unloaded and loaded conditions (50% of subject's body weight) and sagittal 3D T1ρ relaxation time mapping images (MAPSS) were acquired on the index knee. The MR CUBE images were segmented using semi-automatic algorithm with in-house developed MATLAB-based software into ten components including bones, cartilages, menisci, and ligaments, Figure 1. T1ρ maps were reconstructed by fitting the T1ρ-weighted images voxel by voxel to the equation: $S(TSL) \propto \exp(-TSL/T1\rho)$. Segmented cartilage contours were transferred to the T1ρ maps. The subject-specific FE model was developed using FE software LS-Dyna (LSTC) by combining morphological data, in-vivo tissue composition, and axial loading. The human cartilage elasticity (E) was measured using inverse analysis with the equation: $E\,(\text{in MPa}) = \alpha\,(\text{in MPa}) * (1 + (0.86\,\text{s} / T1\rho\,(\text{in s})))/3$. The cartilage material property within each region was assumed to be uniform by using the T1ρ value from the middle part of subregions. Cartilage deformation under the assumed elasticity was compared with MRI measured cartilage deformation.

Results: The results showed that the mean T1ρ value of cMFC-mid was smaller than the cMT-mid, and therefore demonstrated higher stiffness in the medial femoral cartilage (MFC) than in the medical tibial cartilage (MTC). The minimum difference of cartilage deformation between the MR measurement and FE model output was observed as elasticity constant α equals to 3.9 MPa (Fig. 2). Higher pressure distributions and lower maximum contact pressure were found in both femoral cartilage and tibial cartilage with elasticity constant α equals to 3 MPa.

Conclusions: We have built for the first time a FE model that includes subject-specific approximation of the material property of cartilage using in-vivo MRI (T1ρ), and cartilage deformation from loaded MRI was used as a reference to optimize the transformation equation. FE models and loaded MRI measures from more subjects are required to confirm the findings and further optimize the elasticity constant α. In this stud, the mean T1ρ from the defined subcompartment was used. In the future, we may assign voxel-based in-vivo T1ρ values to all FE elements, which however will bring a high computational complexity. The FE model is a powerful tool to detect strain distribution, contact area, and contact pressure within the articular cartilage. Novel imaging